Electron-impact ionization of Li^+

M. S. Pindzola, D. M. Mitnik, and J. Colgan
Department of Physics, Auburn University, Auburn, Alabama 36849

D. C. Griffin
Department of Physics, Rollins College, Winter Park, Florida 32749

(Received 30 November 1999; published 13 April 2000)

Electron-impact ionization cross sections for Li^+ are calculated using the *R* matrix with pseudostates method and time-dependent close-coupling theory. The largest *R*-matrix calculation includes 11 spectroscopic states from the configurations $1s^2$, $1s2l$, and $1s3l$; an additional 56 pseudostates from the configurations $1s\bar{n}\bar{l}$ with $\bar{n}=4-10$ and $l=0-3$; and enough continuum orbitals to adequately describe incident energies up to 175 eV. The largest time-dependent close-coupling calculations involved 16 partial differential equations on a 300 $\times$300 point radial lattice. The nonperturbative *R* matrix with pseudostate and time-dependent close-coupling calculations, as well as perturbative distorted-wave calculations, are in good agreement with the crossed-beams experimental measurements of Lineberger *et al.* [Phys. Rev. **141**, 151 (1966)], but are slightly above the Peart and Dolder [J. Phys. B **2**, 872 (1968)] and Müller *et al.* [Phys. Rev. Lett. **63**, 758 (1989)] measurements.

PACS number(s): 34.80.Dp

I. INTRODUCTION

One of the key atomic collision processes in the modeling of many astrophysical and controlled fusion plasmas is the electron-impact ionization of low-charged ions. The first successful electron ionization measurements were made in the early 1960s on He^+ [1]. Since that time the ionization cross section for hundreds of atomic ions have been measured [2] using a variety of experimental methods. For many atomic ions, the dominant ionization mechanism is the direct ejection of an outer-shell electron by interaction with the passing scattered electron. The final state of the direct mechanism finds two electrons moving in the field of the ionized target, i.e., the quantal three-body Coulomb problem. Since perturbative distorted-wave theory [3] only treats the three-body problem in an approximate fashion, comparison between theory and experiment has been hampered by uncertainties in the perturbative predictions.

Recently a number of computational methods, based on nonperturbative close-coupling theory, have been developed which successfully treat the three-body Coulomb problem found in electron-atom ionization. The converged close-coupling, the *R*-matrix with pseudostates, and the time-dependent close-coupling methods have all been applied to calculate the direct ionization of low-charged atomic ions in Li and Na isoelectronic sequences [4–10]. Although the results from the various computational methods are in reasonably good agreement with each other, the overall agreement between nonperturbative theory and some of the older experiments is less than satisfactory. New experiments on Li-like boron [11] and Na-like aluminum [12] are now in much better agreement with the predictions of the nonperturbative methods.

In this paper, we apply the *R*-matrix with pseudostates and the time-dependent close-coupling methods to the electron ionization of He-like lithium. Crossed-beam experiments [13–15] report ionization cross sections for Li^+ that are well below Coulomb-Born calculations [16], but are in better agreement with distorted-wave with exchange perturbative calculations [17]. Our *R*-matrix with pseudostate calculations extend the recent work of Brown *et al.* [18] by including more pseudostates and by employing procedures to more precisely determine that portion of the pseudo-state expansion that should contribute to ionization. However, since both *R*-matrix calculations only include a sufficiently large $(N+1)$-electron continuum basis to adequately describe incident energies up to about 175 eV, we also carry out time-dependent close-coupling calculations over a larger energy range, which includes the peak of the ionization cross section. The time-dependent method is based on the propagation of a two-electron wave packet in both a nuclear Coulomb potential and an effective local potential for the core electron [19]. Nonperturbative theoretical methods are presented in Sec. II, electron ionization cross sections for Li^+ are presented in Sec. III, and a brief summary is found in Sec. IV.

II. THEORETICAL METHODS

A. *R* matrix with pseudostates

The general *R*-matrix theory for electron-atom collisions [20], and its extension to include pseudostates to represent the continuum [21], is well documented. Our present application to electron ionization is based on the RMATRX I atomic scattering package [22], and the orthogonalization procedure for pseudostate orbitals and continuum box orbitals developed by Gorczyca and Badnell [23]. Bound spectroscopic orbitals for Li^+ were calculated using Froese-Fischer's Hartree-Fock program [24]. The $1s$ orbital was generated from a Hartree-Fock calculation on the $1s^2$ ground configuration, while the $2s$, $2p$, $3s$, $3p$, and $3d$ orbitals were generated from configuration-average Hartree-Fock frozen-core

calculations on the $1s2l$ and $1s3l$ excited configurations. Laguerre-type pseudostates used to represent the highly excited Rydberg states and the N-electron continuum for Li^+ were calculated using Badnell's AUTOSTRUCTURE program [25]. A set of nonorthogonal Laguerre orbitals of the form

$$P_{nl}(r)=N_{nl}(\lambda_l Zr)^{l+1}e^{-\lambda_l Zr/2}L_{n+l}^{2l+1}(\lambda_l Zr) \tag{1}$$

were first generated, where $L_{n+l}^{2l+1}(\lambda_l Zr)$ denotes the associated Laguerre polynomial; N_{nl} is a normalization constant; $Z=z+1$, where z is the residual charge on the ion; and λ_l is a scaling parameter that allows one to adjust the energy and radial extent of the orbitals. These orbitals were then orthogonalized to the Hartree-Fock spectroscopic orbitals and each other.

Two pseudostate expansions were employed: one expansion included the 21 orbitals $\overline{nl}$ ($n=4-10$ and $l=0-2$) from the $1s\overline{nl}$ excited configurations, while the other also included an additional seven orbitals $\overline{nf}$ ($n=4-10$) from the $1s\overline{nf}$ excited configurations. Taking into account total spin angular momentum, the first set of spectroscopic and pseudo-orbitals led to 53 ground and excited LS terms, while the second set of orbitals resulted in a total of 67 LS terms. For both calculations, we employed 40 continuum box orbitals per angular momentum and a box of radius 33.3 a.u. All required $\mathcal{LS}\Pi$ symmetries up to $\mathcal{L}=10$ were included, and they were topped up by using the method described in Badnell *et al.* [8].

The ionization cross section is often determined from the R-matrix with pseudostates method by simply summing up the excitation cross sections to the positive-energy pseudostates. However, pseudostates below the ionization limit contain some continuum character, and those above the ionization limit contain some bound character. We employ the following procedure to more accurately partition the pseudostates between the bound and the continuum. We first adjust the scaling parameters λ_l until the ionization limit lies midway between two term energies for each value of l. We then determine ionization cross sections from the ground state using the equation

$$\sigma_{ion}=\sum_{\overline{n}}\left(1-\sum_{n}|\langle n|\overline{n}\rangle|^2\right)\sigma_{exc}(\overline{n}), \tag{2}$$

where $|\overline{n}\rangle$ denotes a positive or negative-energy pseudostate, $|n\rangle$ denotes a physical discrete state, and $\sigma_{exc}(\overline{n})$ is the excitation cross section from the ground state to $|\overline{n}\rangle$. In practice, after the scaling parameters have been adjusted as described above, the difference in determining the ionization cross section using Eq. (2) and just summing over all excitation to positive-energy pseudostates is on the order of 5%.

The most time-consuming part of this calculation is the diagonalization of the $(N+1)$-electron Hamiltonian. The 67-state calculation required the diagonalization of dense matrices up to a rank of 6749. In order to extend these calculations to higher energy, we would have been forced to include more pseudostates to accurately represent the N-electron continuum, and a much larger set of box orbitals to represent the $(N+1)$-electron continuum; this would have in turn greatly increased the rank of the matrices to be diagonalized.

B. Time-dependent close-coupling theory

The time-dependent close-coupling theory for electron-atom collisions is set forth in studies of the electron-impact ionization of hydrogen [26,27]. The extension of the formulation to calculate the electron-impact ionization of helium [19] may be directly applied to the ionization of Li^+. A frozen-core $1s$ orbital is calculated as the hydrogenic ground state of Li^{2+}. A set of radial orbitals $\overline{nl}$ are obtained by diagonalization of the Hamiltonian given by

$$h(r)=-\frac{1}{2}\frac{\partial^2}{\partial r^2}+\frac{l(l+1)}{2r^2}-\frac{Z_t}{r}+V_H(r)+V_X(r), \tag{3}$$

where $Z_t=3$, $V_D(r)$ is the direct Hartree potential, and $V_X(r)$ is a local exchange potential. Both the direct and exchange potentials are calculated using the frozen-core $1s$ orbital. A parameter in the exchange term is adjusted so that the single particle energies for each angular momentum are in reasonable agreement with the configuration-average experimental spectrum. The $\overline{1s}$ orbital has an energy of $\epsilon_{\overline{1s}}=-75.6$ eV, and is very similar to the Hartree-Fock ground state radial orbital of Li^+.

At a time $t=0$ before the collision, two-electron radial wave functions $P_{l_1l_2}^{LS}(r_1,r_2,t)$ are given by antisymmetrized products of the $\overline{1s}$ orbital and an incoming radial wave packet. Their propagation in time is governed by the Schrödinger equation, which takes the form of a set of time-dependent close-coupled partial differential equations for each LS symmetry given by

$$i\frac{\partial P_{l_1l_2}^{LS}(r_1,r_2,t)}{\partial t}=T_{l_1l_2}(r_1,r_2)P_{l_1l_2}^{LS}(r_1,r_2,t)+\sum_{l_1',l_2'}U_{l_1l_2,l_1'l_2'}^{L}(r_1,r_2)P_{l_1'l_2'}^{LS}(r_1,r_2,t), \tag{4}$$

where $T_{l_1l_2}(r_1,r_2)$ contains kinetic energy, centrifugal barrier, nuclear, direct Hartree, and local exchange operators, and $U_{l_1l_2,l_1'l_2'}^{L}(r_1,r_2)$ couples the various (l_1l_2) scattering channels [19]. At a time $t=T$ following the collision, the two-electron radial wave functions are projected onto products of the $\overline{nl}$ orbitals to extract collision probabilities and thus inelastic cross sections.

For electron ionization of Li^+ the time-dependent close-coupling equations [see Eq. (4)] for the two-electron radial wave functions are solved on two different numerical lat-

TABLE I. Partial ionization cross sections (10^{-18} cm^2) for Li^+ at an incident electron energy of 150 eV ($\mathcal{L}$ is the total angular momentum).

$\mathcal{L}$	Distorted wave no exchange	Distorted wave with exchange	R matrix 53 states	R matrix 67 states	Wave packet $\Delta r=0.20$	Wave packet $\Delta r=0.15$
0	0.386	0.320	0.291	0.292	0.326	0.308
1	0.506	0.426	0.497	0.497	0.533	0.501
2	1.495	1.232	1.056	1.032	1.062	1.016
3	1.070	0.868	0.858	0.855	0.828	0.811
4	0.611	0.509	0.502	0.521	0.479	0.477
5	0.311	0.269	0.257	0.260	0.237	0.238
6	0.148	0.133	0.116	0.119	0.112	0.113
7-30	0.122	0.118				

tices. One lattice has 200×200 points, with each radial direction from 0 to 40 a.u. spanned by a uniform mesh with spacing $\Delta r=0.20$ a.u., while a second lattice has 300×300 points with each radial direction from 0 to 45 a.u. spanned by a uniform mesh with spacing $\Delta r=0.15$ a.u. The number of $(l_1 l_2)$ coupled channels ranges from 4 for $^{1,3}S$ to 16 for $^{1,3}I$ symmetry. The total time propagation of the radial wave functions is determined by the convergence of the collision probabilities. Generally, shorter times are needed for larger incident energies.

C. Distorted-wave theory

The distorted-wave theory for electron-impact ionization of atoms is based on a triple partial-wave expansion of the first-order perturbation theory scattering amplitude [3]. The $1s$ orbital for Li^+ is generated from a Hartree-Fock calculation on the $1s^2$ ground configuration. The incident and scattered electrons are calculated in a V^N potential, while the ejected electron is calculated in a V^{N-1} potential, where $N=2$ is the number of electrons on the target. Two distorted-wave calculations for the electron ionization of Li^+ are made: one includes only the direct term in the scattering amplitude, while the second includes both direct and exchange terms.

III. RESULTS

Partial-wave ionization cross sections for electron scattering from Li^+ at an incident energy of 150 eV, calculated in the perturbative distorted-wave, the nonperturbative R-matrix with pseudostates, and time-dependent wave-packet methods are presented in Table I. The overall agreement between the perturbative and nonperturbative calculations is reasonably good. For example, all the calculations predict a maximum in the partial cross sections at $\mathcal{L}=2$. The R-matrix results for the partial cross sections given here are obtained by summing over all excitation to the positive energy pseudostates, while the correction given by Eq. (2) lowers the total cross section by about 5%. By $\mathcal{L}=6$, the partial cross sections determined from the 67-state R-matrix calculation and the most accurate time-dependent calculation differ by only 5%; furthermore, the partial cross section determined from the distorted-wave with exchange method is only 12% higher than the 67-state R-matrix result and 18% higher than the most accurate time-dependent result.

Total ionization cross sections for electron scattering from Li^+ at low incident energies are presented in Fig. 1. The dashed curve gives the 67-state R-matrix results convolved with an 2.0-eV Gaussian to smooth out the narrow pseudoresonance structure, while the solid curve is obtained from a fourth-degree polynomial fit through the remaining pseudoresonance oscillations. The R-matrix ionization cross sections are determined using Eq. (1). The 53-state R-matrix results, which are not shown in Fig. 1, are in excellent agreement with the 67-state R-matrix results between threshold and 150 eV; however, the two calculations begin to differ more appreciably at about 175 eV. The open square at 150 eV gives the time-dependent close-coupling results for $\mathcal{L}=0-6$ combined with the distorted-wave with exchange results for $\mathcal{L}=7-30$. The wave-packet results are for the 300×300 lattice; the 200×200 lattice results are 3.2% higher.

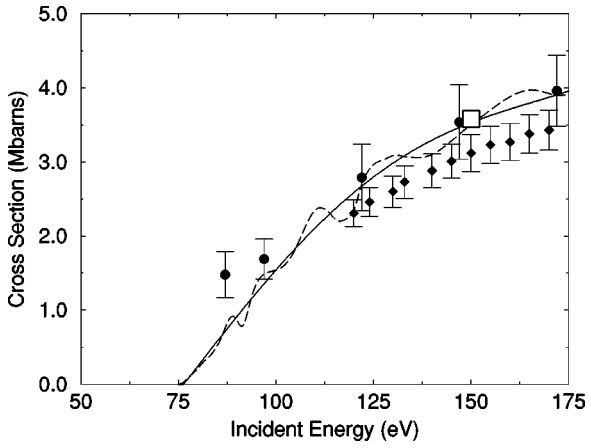

FIG. 1. Total electron-impact ionization cross section for Li^+. Dashed curve: 67-state R matrix with pseudostates method. Solid curve: fourth-degree polynomial fit to the 67-state R-matrix with pseudostate calculation. Open square: time-dependent close-coupling method, topped up at high angular momentum with distorted-wave results. Solid circles: experimental measurements [13]. Solid diamonds: experimental measurements [15] (1.0 Mbarn$=1.0\times10^{-18}$ cm^2).

TABLE II. Partial ionization cross sections (10^{-18} cm^2) for Li^+ at an incident electron energy of 250 eV ($\mathcal{L}$ is the total angular momentum).

$\mathcal{L}$	Distorted wave no exchange	Distorted wave with exchange	Wave packet $\Delta r=0.20$	Wave packet $\Delta r=0.15$
0	0.302	0.242	0.283	0.258
1	0.453	0.365	0.498	0.452
2	1.062	0.861	0.870	0.818
3	1.118	0.918	0.915	0.878
4	0.913	0.774	0.753	0.737
5	0.654	0.576	0.531	0.529
6	0.436	0.398	0.349	0.353
7-30	0.750	0.738		

We note that the ''top up'' in angular momentum coming from the distorted-wave with exchange calculations is only 3.3% of the total ionization cross section at 150 eV. The solid circles and solid diamonds are crossed-beam experimental measurements [13,15]. We find that the *R*-matrix pseudostate and time-dependent close-coupling calculations are in excellent agreement with each other and with the experimental measurements of Lineberger *et al.* [13] over this energy range, but above the top of the error bars in regard to the measurements of Müller *et al.* [15]. On the other hand, the 45-state *ab initio R*-matrix calculations of Brown *et al.* [18] are 15–20 % lower than the *R*-matrix and wave-packet results shown in Fig. 1, but are within the error bars of the measurements of Müller *et al.* [15].

Partial-wave ionization cross sections for electron scattering from Li^+ at incident energies of 250 and 400 eV, calculated in the perturbative distorted-wave and nonperturbative wave-packet methods, are presented in Tables II and III. The accuracy of the perturbative calculations should improve at the higher angular momentum and higher incident energies. For example, the wave packet $\mathcal{L}=6$ partial cross sections are 11% lower than the distorted-wave with exchange results at 250 eV, and 4% lower at 400 eV.

Total ionization cross sections for electron scattering from Li^+ at intermediate incident energies are presented in Fig. 2.

TABLE III. Partial ionization cross sections (10^{-18} cm^2) for Li^+ at an incident electron energy of 400 eV ($\mathcal{L}$ is the total angular momentum).

$\mathcal{L}$	Distorted wave no exchange	Distorted wave with exchange	Wave packet $\Delta r=0.20$	Wave packet $\Delta r=0.15$
0	0.175	0.140	0.202	0.173
1	0.302	0.240	0.375	0.322
2	0.606	0.492	0.575	0.526
3	0.746	0.621	0.689	0.642
4	0.733	0.629	0.671	0.638
5	0.632	0.562	0.569	0.553
6	0.504	0.463	0.448	0.444
7-30	1.445	1.432		

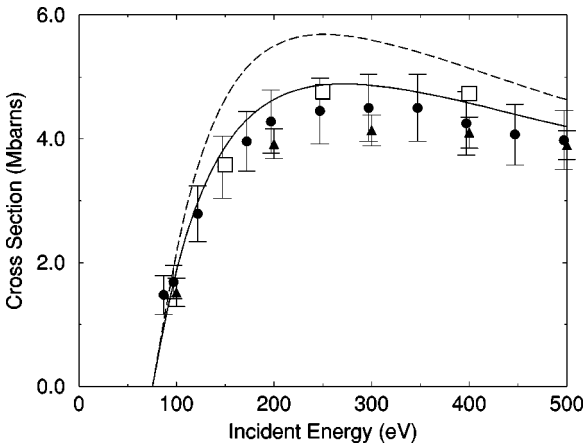

FIG. 2. Total electron-impact ionization cross section for Li^+. Open squares: time-dependent close-coupling method, topped up at high angular momentum with distorted-wave results. Solid curve: distorted-wave with exchange method. Dashed curve: distorted-wave no exchange method. Solid circles: experimental measurements [13]. Solid triangles: experimental measurements [14] (1.0 Mbarn$=1.0\times10^{-18}$ cm^2).

The open squares give the time-dependent close-coupling results for $\mathcal{L}=0-6$ combined with the distorted-wave with exchange results for $\mathcal{L}=7-30$. The wave-packet results are for the 300×300 lattice; the 200×200 lattice results are from 3% to 5% higher. We note that the ''top up'' in angular momentum coming from the distorted-wave with exchange calculations has increased to 30% of the total ionization cross section by 400 eV. The solid curve gives the distorted-wave with exchange results, while the dashed curve gives the distorted-wave no-exchange results. The distorted-wave with exchange calculations by Younger [17] are in excellent agreement with those shown in Fig. 2, while the Coulomb-Born calculations of Moores and Nussbaumer [16] agree well with the distorted-wave no-exchange results. The solid circles and solid triangles are crossed-beams experimental measurements [13,14]. We find that, at higher energies, the time-dependent close-coupling calculations are somewhat above the experimental measurements of Lineberger *et al.* [13], but well within the error bars; however, they are above the top of the error bars for the measurements of Peart and Dolder [14]. We note that the distorted-wave with exchange results are also within the error bars of the measurements of Lineberger *et al.* [13].

IV. SUMMARY

The *R*-matrix pseudostate and time-dependent close-coupling methods have been applied to calculate the electron-impact ionization cross section for Li^+. Both of these nonperturbative methods seem to confirm the overall accuracy of previous perturbative distorted-wave calculations [17]; they are somewhat higher, but also in reasonably good agreement with previous experimental measurements [13–15].

Based on the present work for Li^+, we expect that the distorted-wave with exchange method can be used to accurately predict the electron-impact ionization cross section from the ground state for all positively charged atomic ions in the helium isoelectronic sequence. In the future we hope to extend nonperturbative electron scattering theory to examine the ionization process in other open- and closed-shell atomic systems.

ACKNOWLEDGMENTS

We would like to thank Dr. Nigel Badnell and Dr. Francis Robicheaux for several useful discussions. This work was supported in part by the U.S. Department of Energy under Grant No. DE-FG05-96-ER54348 with Auburn University. Computational work was carried out at the National Energy Research Supercomputer Center in Berkeley, California.

[1] K. T. Dolder, M. F. A. Harrison, and P. C. Thonemann, Proc. R. Soc. London, Ser. A **264**, 367 (1961).
[2] H. Tawara and M. Kato, NIFS-DATA-51, 1 (1999).
[3] S. M. Younger, in *Electron Impact Ionization*, edited by T. D. Mark and G. H. Dunn (Springer-Verlag, Berlin, 1985), p. 1.
[4] I. Bray, J. Phys. B **28**, L247 (1995).
[5] K. Bartschat and I. Bray, J. Phys. B **30**, L109 (1997).
[6] M. S. Pindzola, F. Robicheaux, N. R. Badnell, and T. W. Gorczyca, Phys. Rev. A **56**, 1994 (1997).
[7] P. J. Marchalant, K. Bartschat, and I. Bray, J. Phys. B **30**, L435 (1997).
[8] N. R. Badnell, M. S. Pindzola, I. Bray, and D. C. Griffin, J. Phys. B **31**, 911 (1998).
[9] D. M. Mitnik, M. S. Pindzola, D. C. Griffin, and N. R. Badnell, J. Phys. B **32**, L479 (1999).
[10] M. P. Scott, H. Teng, and P. G. Burke, J. Phys. B **33**, 463 (2000).
[11] O. Woitke, N. Djuric, G. H. Dunn, M. E. Bannister, A. C. H. Smith, B. Wallbank, N. R. Badnell, and M. S. Pindzola, Phys. Rev. A **58**, 4512 (1998).
[12] J. W. G. Thomason and B. Peart, J. Phys. B **31**, L201 (1998).
[13] W. C. Lineberger, J. W. Hooper, and E. W. McDaniel, Phys. Rev. **141**, 151 (1966).
[14] B. Peart and K. T. Dolder, J. Phys. B **2**, 872 (1968).
[15] A. Müller, G. Hofmann, B. Weissbecker, M. Stenke, K. Tinschert, M. Wagner, and E. Salzborn, Phys. Rev. Lett. **63**, 758 (1989).
[16] D. L. Moores and H. Nussbaumer, J. Phys. B **3**, 161 (1970).
[17] S. M. Younger, Phys. Rev. A **22**, 1425 (1980).
[18] G. J. N. Brown, M. P. Scott, and K. A. Berrington, J. Phys. B **32**, 737 (1999).
[19] M. S. Pindzola and F. J. Robicheaux, Phys. Rev. A **61**, 052707 (2000).
[20] P. G. Burke and K. A. Berrington, *Atomic and Molecular Processes: an R-matrix Approach* (Institute of Physics, Bristol, 1993).
[21] K. Bartschat, Comput. Phys. Commun. **114**, 168 (1998).
[22] K. A. Berrington, W. B. Eissner, and P. H. Norrington, Comput. Phys. Commun. **92**, 290 (1995).
[23] T. W. Gorczyca and N. R. Badnell, J. Phys. B **30**, 3897 (1997).
[24] C. Froese-Fischer, Comput. Phys. Commun. **43**, 355 (1987).
[25] N. R. Badnell, J. Phys. B **19**, 3827 (1986).
[26] M. S. Pindzola and D. R. Schultz, Phys. Rev. A **53**, 1525 (1996).
[27] M. S. Pindzola and F. Robicheaux, Phys. Rev. A **54**, 2142 (1996).